Significant mechanical interactions at physiological lengths and relative positions of rat plantar flexors

Bernabei, M.; van Dieen, J.H.; Baan, G.C.; Maas, H.

published in
Journal of Applied Physiology (1985)
2015

DOI (link to publisher)
10.1152/japplphysiol.00703.2014

Significant mechanical interactions at physiological lengths and relative positions of rat plantar flexors

Michel Bernabei, Jaap H. van Dieën, Guus C. Baan and Huub Maas

J Appl Physiol 118:427-436, 2015. First published 24 December 2014;
doi:10.1152/japplphysiol.00703.2014

Journal of Applied Physiology publishes original papers that deal with diverse areas of research in applied physiology, especially those papers emphasizing adaptive and integrative mechanisms. It is published 12 times a year (monthly) by the American Physiological Society, 9650 Rockville Pike, Bethesda MD 20814-3991. ISSN: 0363-6143, ESSN: 1522-1563. Visit our website at http://www.the-aps.org/.

J Appl Physiol 118: 427–436, 2015.
First published December 24, 2014; doi:10.1152/japplphysiol.00703.2014.

Significant mechanical interactions at physiological lengths and relative positions of rat plantar flexors

Michel Bernabei, Jaap H. van Dieën, Guus C. Baan, and Huub Maas

Research Institute MOVE, Faculty of Human Movement Sciences, VU University Amsterdam, The Netherlands

Submitted 5 August 2014; accepted in final form 21 December 2014

Bernabei M, van Dieën JH, Baan GC, Maas H. Significant mechanical interactions at physiological lengths and relative positions of rat plantar flexors. *J Appl Physiol* 118: 427–436, 2015. First published December 24, 2014; doi:10.1152/japplphysiol.00703.2014.—In situ studies involving supraphysiological muscle lengths and relative positions have shown that connective tissue linkages connecting adjacent muscles can transmit substantial forces, but the physiological significance is still subject to debate. The present study investigates effects of such epimuscular myofascial force transmission in the rat calf muscles. Unlike previous approaches, we quantified the mechanical interaction between the soleus (SO) and the lateral gastrocnemius and plantaris complex (LG+PL) applying a set of muscle lengths and relative positions corresponding to the range of knee and ankle angles occurring during normal movements. In nine deeply anesthetized Wistar rats, the superficial posterior crural compartment was exposed, and distal and proximal tendons of LG+PL and the distal SO tendon were severed and connected to force transducers. The target muscles were excited simultaneously. We found that SO active and passive tendon force was substantially affected by proximally lengthening of LG+PL mimicking knee extension (10% and 0.8% of maximal active SO force, respectively; $P < 0.05$). Moreover, SO relative position significantly changed the LG+PL length-force relationship, resulting in nonunique values for passive slack-length and optimum-length estimates. We conclude that also, for physiological muscle conditions, isometric force of rat triceps surae muscles is determined by its muscle-tendon unit length as well as by the length and relative position of its synergists. This has implications for understanding the neuromechanics of skeletal muscle in normal and pathological conditions, as well as for studies relying on the assumption that muscles act as independent force actuators.

myofascial force transmission; connective tissue; soleus muscle; passive slack length; length-force characteristics

IN THE LAST DECADE, epimuscular myofascial force transmission (EMFT) has been revealed as a codeterminant of isometric muscle force (16–17, 36, 45). The myofascial pathway, connecting the epimysium of a muscle to surrounding structures, has been proven to serve as a secondary pathway for transmitting muscle force besides the well-known myotendinous pathway. This perspective of musculoskeletal organization challenges the concept of muscles as independent actuators. Despite the anatomical and experimental evidence reported in a number of in situ animal studies (16) and intraoperative studies in humans (26, 52), the functional relevance of EMFT is still subject of considerable debate (9, 35).

Several in situ animal studies have reported clear evidence of EMFT (16, 36). Significant differences between forces exerted at the proximal and distal tendons of the same muscle have been found in the rat hindlimb (e.g., Ref. 31). A change in muscle length was found to result not only in a force change at the tendons of the lengthened muscle but also in a change of the force exerted at the proximal and distal tendons of synergistic muscles (18, 32). However, in those studies muscle lengths and relative positions were in many conditions beyond physiological. In addition to animal studies, several groups have investigated EMFT between triceps surae muscles in humans by using local strain maps estimated from MRI and ultrasound imaging of triceps surae muscles (4, 21, 55, 62). They confirmed the presence of intermuscular interaction in vivo by showing that imposing global strains on gastrocnemius muscle resulted also in tissue displacements or length changes of its synergistic soleus (SO). However, tissue deformations do not provide a direct measure of force transmission. In contrast, no significant mechanical interactions between SO and gastrocnemius were observed in the cat when physiological ranges of lengthening were imposed through joint movement (35). As the mechanical effect of SO was assessed by the ankle joint moment it exerted, no information about individual tendon forces is available. Moreover, indirect muscle force estimation from recorded joint moments does not allow to discriminate between intermuscular effects of common elasticity mediated by the Achilles tendon and effects of EMFT; each mechanism may change SO muscle force in opposite direction (49, 56). Finally, only the muscle of interest (i.e., SO) was excited, whereas in the rat studies described above, several synergistic and antagonistic muscles were activated.

Most biomechanical models that describe the human musculoskeletal system assume that muscles transmit forces only via myotendinous pathways, with muscles thus acting as independent actuators (e.g., Refs. 3, 14, 29, 56). Such an assumption is fundamental when mechanical characteristics of individual muscles are estimated in humans (10, 60). A method first presented to estimate active muscle force in the 1980s (11, 22) and subsequently extended for estimation of passive muscle force (12) is currently widely used to determine the length-force characteristics of human biarticular muscles in vivo (38, 42). Briefly, if all the synergists and antagonists of a biarticular muscle span one joint only, their contribution to the shared-joint net moment would be constant for any given angle of the other joint. The implicit assumption is that the net joint moment of a biarticular muscle can be linearly reconstructed by summing the contribution of synergistic muscles, the muscle-tendon unit (MTU) length being the only determinant of isometric muscle force. If EMFT is of significance in physiological conditions, this assumption is not valid.

The primary aim of the present study was to quantify the transmission of force between rat plantar flexor muscles within a physiological range of muscle lengths and relative positions corresponding to knee and ankle angles occurring during normal movement. We hypothesized that the effects of EMFT

Address for reprint requests and other correspondence: H. Maas, Van der Boechorststraat 9, 1081 Amsterdam, The Netherlands (e-mail: h.maas@vu.nl).

found in previous studies will also be of importance within a physiological range of MTU lengths and relative positions. For this purpose, we measured isometric forces exerted at the proximal and distal tendons of lateral gastrocnemius (LG) and plantaris (PL) complex (LG+PL) as well as at the distal tendon of SO muscle, while activating the synergistic muscle group simultaneously. The secondary aim of this study was to assess the extent of EMFT effects on LG+PL length-force characteristics and derived parametric estimates, such as maximum isometric force, MTU slack, and optimum lengths.

METHODS

Animal Conditions

Experiments were performed on nine male Wistar rats (body mass 311.1 ± 4.5 g). All surgical and experimental procedures were approved by the Committee on the Ethics of Animal Experimentation at the VU University Amsterdam and in strict agreement with the guidelines and regulations concerning animal welfare and experimentation set forth by Dutch law.

According to standard procedures in our laboratory (e.g., Ref. 31) the animals were anesthetized by an intraperitoneal injection of urethane solution (1.2 ml/100 g body mass, 12.5% urethane solution). Extra doses were administered if necessary (1.5 ml maximally) until withdrawal reflexes to a pain stimulus were suppressed completely. Body temperature was controlled by a rectal thermometer and maintained at ~37°C during surgery and data collection by adjusting the temperature of an electrical heating pad. A controlled air conditioning system kept ambient temperature and air humidity at a constant level (22° and 70%, respectively). Regular irrigation with isotonic saline prevented dehydration of exposed tissues. At the end of the measurements, the animals were euthanized with a pentobarbital (Euthasol 20%) overdose injected intracardially, followed by double-sided pneumothorax.

Surgical Procedures

The skin and most of the biceps femoris muscle covering the dorsal side of the left hindlimb were removed to expose the superficial posterior crural compartment, which contains SO, LG, medial gastrocnemius, and PL muscles. Both the LG and PL originate from the lateral epicondyle of the femur, with their proximal tendons merged and twisted together. Medial gastrocnemius was excised fully by resecting its distal tendon from the Achilles tendon and carefully cutting the muscle fibers that insert onto the medial side of its distal aponeurosis, which is shared with the LG. The SO, LG, PL muscle group was dissected free from surrounding structures, preserving the bone insertions, as well as the connective tissue linkages and the neurovascular tract at the interface between the SO and LG+PL muscle bellies. Intermuscular connective tissues between the SO and LG+PL muscle bellies was found both proximally and distally of the neurovascular tract, which runs centrally between SO and LG muscle bellies (Fig. 1). Intermuscular linkages between the SO and PL muscles were found deeper in the dorsal compartment, along the medial edge of SO.

A bipolar cuff electrode connected to a constant current source (Digitimer DS3, Digitimer, Hertfordshire, UK) was folded around the sciatic nerve. The peroneal nerve, innervating the muscles in the peroneal and anterior crural compartments, was severed. With the hindlimb held in the reference position P_{ref} (i.e., ankle and knee joints at 90°; included angles between the adjacent segments), markers were placed on the distal tendon of SO, on the proximal and distal tendons of LG+PL, and on two fixed locations in the tibial compartment (Fig. 2). These were used to identify the position of the distal tendons corresponding to P_{ref} for the ankle angle at 90° (P^{A}_{ref}) and the position of the LG+PL proximal tendon corresponding to P_{ref} for the knee angle at 90° (P^{K}_{ref}) and to apply MTU length changes relatively to the reference positions (ΔP) during data collection. The reference length (L_{ref}) is then defined as the MTU length at the reference position P_{ref}. The reference length for the SO ($L_{ref,SO}$) depends only on distal tendon position, whereas the reference length for LG+PL ($L_{ref,LG+PL}$) depends on the position of both proximal and distal LG+PL tendons.

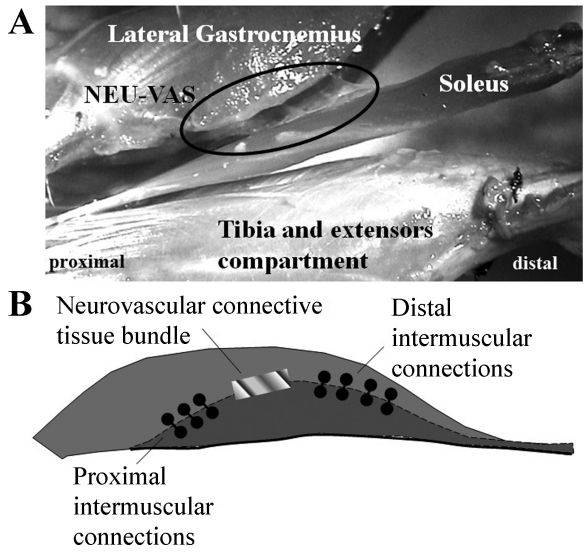

Fig. 1. Intermuscular and extramuscular connections of soleus (SO). *A*: lateral view of the neurovascular tract (NEU-VAS) embedding the nerves and blood vessels for SO muscle. This tract runs from the ventral side of lateral gastrocnemius (LG) to the dorsal side of SO muscle belly. The picture was taken after collection of force data, following disruption of the intermuscular connective tissues at the interface between SO and LG and plantaris complex (LG+PL) muscles. The LG+PL was pulled in proximoposterior direction and the SO distally to make the tract visible. *B*: schematic overview of the connective tissue linkages observed between the SO and LG+PL. Intermuscular connections are present at the whole interface between SO (dark gray) and LG (light gray) proximally and distally of the neurovascular tract (represented by lines crossing the interface).

The distal SO tendon was carefully dissected free from the rest of the Achilles tendon and subsequently cut and connected to a force transducer (ALPHA load beam transducer, 25 N maximum capacity, maximum output error <0.1%, compliance 0.0162 mm/N; BLH Electronics, Toronto, Canada) with Kevlar thread. The proximal and distal tendons of the LG+PL complex were freed from the skeleton by cutting a small bone fragment from the lateral femoral condyle and from the calcaneus, respectively, and then connected to force transducers (Z6 bending beam load cell, 50 N maximum capacity, maximum output error <0.1%, compliance 0.0048 mm/N; HBM, Darmstadt, Germany) with Kevlar thread. Similar to a previous study (31), we confirmed that force differences between the proximal and distal tendon of LG+PL greater than $1.2 \cdot 10^{-3}$ N cannot be ascribed to the measurement system. Force transducers were positioned in such a way that forces could be measured in the muscle's line of pull, and that the relative position of the muscles and tendons mimicked that of the in vivo situation. For each contraction, the whole hindlimb of the rat was videotaped (DCR-TRV6E, 2000 Sony; 720 × 576 pixels, 25 fps).

Nerve stimulation. The sciatic nerve was stimulated supramaximally (0.4 ± 0.1 mA, 500 ms, 100 Hz), eliciting a tetanic contraction of LG, PL, and SO simultaneously. Two twitches were evoked before each contraction to enable the muscles to adapt to the imposed length and relative position. A 2-min recovery time was allowed in between subsequent stimulations. Nerve stimulation, force signal acquisition, and A/D conversion were controlled and sequenced by using a data acquisition board (PCI-6221, National Instruments, Austin, TX).

Experimental protocol. Before acquiring data, multiple (~10–15) contractions at high and low lengths were performed to minimize

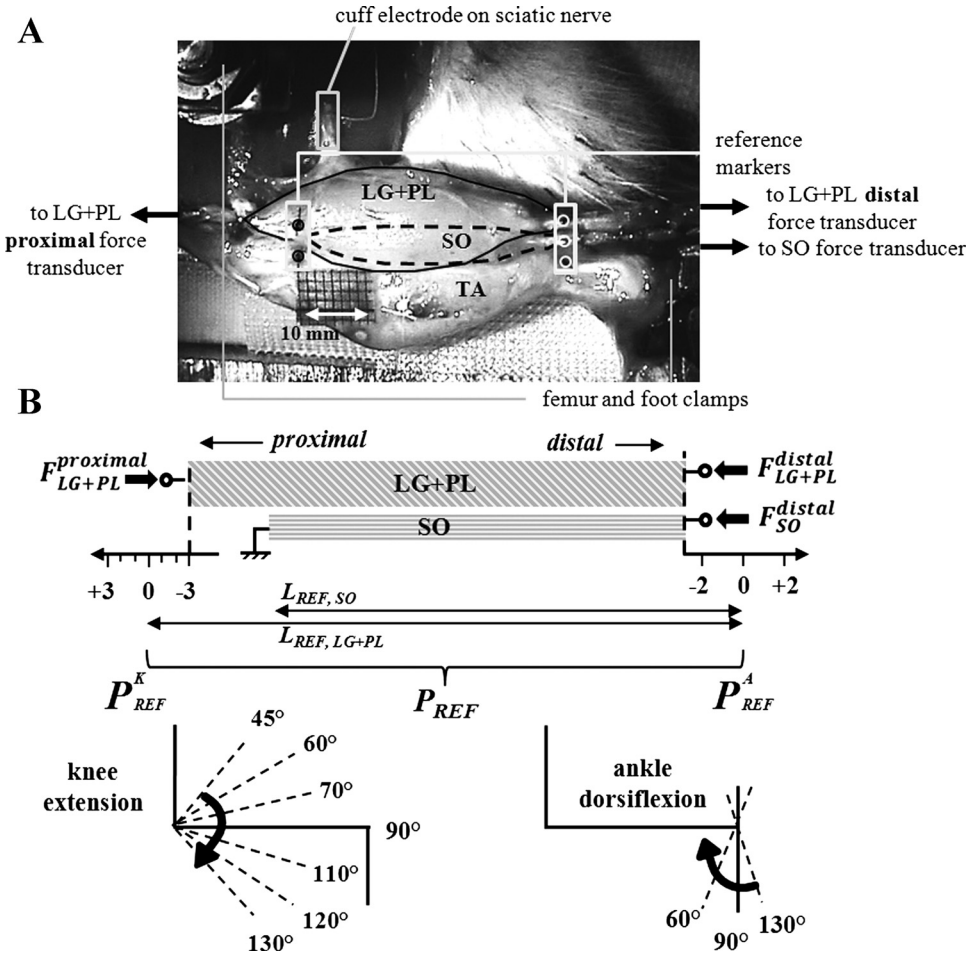

Fig. 2. Experimental setup and protocol. *A*: rat hindlimb in the experimental setup. Proximal and distal tendons of LG+PL as well as the distal tendon of SO were connected to separate force transducers. The femur was fixed with a metal clamp and the foot with a plastic plate. A bipolar cuff electrode was placed on the sciatic nerve. The reference markers (proximal: black circles; distal: white circles) applied on the tendons and on the anterior tibial compartment identified the reference position (P_{ref}), i.e., the muscle-tendon unit (MTU) length corresponding to a 90–90° knee-ankle joint-configuration. *B*: experimental protocol. The applied positional changes for distal LG+PL tendons and SO tendons ($P^{K}_{ref}-3$ to $P^{K}_{ref}+3$ mm corresponding to 45 to 130° knee extension and $P^{A}_{ref}-2$ to $P^{A}_{ref}+2$ mm corresponding to 130 to 60° ankle dorsiflexion). Distal SO and distal LG+PL tendons were always repositioned together and in equal steps.

history effects (18). Isometric forces exerted at all three tendons were measured simultaneously for different lengths and relative positions of LG+PL and SO muscles. These were selected based on ankle and knee joint angles observed during normal movements, such as walking, swimming, ladder walking, and trotting (2, 5, 7, 39). Changes in MTU length corresponding to those joint angles were assessed via a musculoskeletal model of the rat hindlimb (23). The experiment consisted of the two following set of imposed muscle lengths and relative positions.

Length-force characteristics of SO and LG+PL complex. The proximal LG+PL tendon was kept at P^{K}_{ref} ($\Delta P = 0$ mm LG+PL proximal displacement from P_{ref}). The distal LG+PL and SO tendons were repositioned together in steps of 1 mm from -2 mm below P^{A}_{ref} increasing to ~1 mm over SO optimum length, which was found at a smaller displacement of the distal tendon than optimum length of LG+PL. To prevent possible damage to SO, the muscles were not lengthened any further, and thus LG+PL optimum length was not included in the data set.

SO and LG+PL forces at different positions of LG+PL proximal tendon. Length changes of LG+PL without length changes of SO were obtained by repositioning the proximal LG+PL tendon exclusively. In steps of 1 mm, LG+PL was lengthened from $P^{K}_{ref}-3$ mm, corresponding to ~45° knee angle, to $P^{K}_{ref}+3$ mm, corresponding to ~130° knee angle (Fig. 2). Effects of such length changes of LG+PL proximally were assessed for three different positions of the distal tendons of LG+PL and SO, i.e., from $P^{A}_{ref}-2$ mm (corresponding to ~130° ankle angle) to $P^{A}_{ref}+2$ mm (corresponding to ~60° ankle angle). The distal tendons of LG+PL and SO were always repositioned together and in equal steps. This resembles the natural condition in which those muscles have a similar moment arm at the ankle joint (23, 35).

Data Analysis and Statistics

Isometric forces were assessed from the force-time series: passive force (F_P) was assessed by calculating the mean for a 50-ms time window before the tetanic contraction and total force was assessed by calculating the mean for the 50 ms before the end of the tetanic contraction. Active force (F_A) was calculated as the difference between total and passive force at equal MTU length and relative position. SO and LG+PL MTU lengths were expressed as the deviation (ΔP_{SO}, ΔP_{LG+PL}) from the length at P_{ref}. MTU length of LG+PL at P_{ref} was assessed with the video images from ImageJ software (v. 1.46b, National Institutes of Health, Bethesda, MD). SO MTU length could not be assessed because the SO proximal tendon is covered by the LG+PL muscle bellies.

Length-force characteristics obtained from *protocol 1* were superimposed at optimum length of SO and then averaged across animals. Active forces were fitted with a third order polynomial (37) because only five MTU lengths were measured. For each LG+PL proximal position (P^{K}_{LG+PL}) imposed with the second protocol, passive and active forces exerted at the SO distal tendon were (without any fitting) averaged, yielding three curves, each corresponding to a different simulated ankle configuration (130, 90, 60°). Two different measures of mechanical interaction among the triceps surae muscles were obtained from the second protocol: *1*) changes in SO force as a result of proximal LG+PL length changes and *2*) LG+PL forces measured at the same MTU length but with a different length and relative position of SO. The latter measure of mechanical interaction provides three data points of LG+PL proximal and distal forces at equal MTU length, but with different lengths and relative positions of the SO muscle.

LG+PL length-passive force data obtained from the second protocol were fitted with an exponential function as proposed by Hoang et al. (12) (Fig. 3):

$$F_P = a_g * \left(e^{k_g(x-L_g)} - 1\right) \quad (1)$$

where a_g, k_g and L_g are the three constants estimated by nonlinear least square method. According to Hoang's method, L_g provides the estimate for LG+PL passive slack length. However, it was not always possible to calculate a plausible estimate of the passive slack length based only on L_g because the fitted passive length-force curve did not always cross the zero-force level when extrapolating toward lower muscle lengths. Therefore, we used a $5*10^{-5}$ N/mm threshold (~0.05% of the mean maximal passive force) on the derivative of the passive length-force function to estimate slack length for each animal and condition (Fig. 3, vertical dashed lines).

The three LG+PL length-active force data sets obtained from the second protocol were each fitted with a fourth order polynomial function by using a nonlinear least squares criterion. Maximal active force and the corresponding optimum length were estimated for each of the active-force curves. The ranges of variation between passive as well as active fitted curves were assessed by calculating root mean square errors (RMSE) for the full range of LG+PL lengths tested (i.e., 10 mm MTU length range). This analysis for passive and active forces was applied to both proximally and distally exerted force of LG+PL. Ranges of variation between estimates were calculated for each animal and expressed as a percentage of the mean estimated value among the three different SO relative positions. Also, differences between estimates based on proximal rather than distal LG+PL tendon forces were assessed.

Two-way ANOVA for repeated measures (factors: position of SO+LG+PL distal tendons and location of LG+PL force measurement) was performed to test for differences between the force in proximal and distal tendons of LG+PL when repositioning SO+LG+PL distal tendons together. Two-way ANOVA for repeated measures (factors: position of LG+PL proximal tendon and position of SO+LG+PL distal tendons) was used to test for effects of repositioning the proximal tendon of LG+PL on active and passive forces exerted at the distal SO tendon. Two-way ANOVA for repeated measures (factors: LG+PL length and SO relative position) was also performed to compare LG+PL active and passive isometric forces measured at the same LG+PL MTU-length, but with a different SO muscle relative position. When a significant main effect was found, Bonferroni post hoc pairwise comparisons were used to assess at which muscle lengths force differences were significant ($P < 0.05$).

RESULTS

Length-Force Characteristics of SO and LG+PL Complex

SO maximal active force (1.47 ± 0.06 N) was found for a SO MTU length of 1.9 ± 1.4 mm beyond $L_{ref,SO}$, whereas SO force at $L_{ref,SO}$ was 1.35 ± 0.07 N (Fig. 4*A*). SO passive forces were near zero at $L_{ref,SO}$ (0.009 ± 0.006 N) and 0.023 ± 0.009 N at optimum length. At the reference position, MTU length of LG+PL was 43.2 ± 2.5 mm, whereas LG+PL active force was 11.8 ± 1.5 N at the proximal tendon and 11.9 ± 1.5 N at the distal tendon. Within the applied length range for LG+PL, no optimum length was found. Proximally and distally measured LG+PL passive forces at $L_{ref,LG+PL}$ were 0.141 ± 0.058 N and 0.155 ± 0.045 N, respectively. Neither for passive nor for active force were forces exerted at the proximal tendon of LG+PL significantly different from those exerted at the distal tendon (Fig. 4*B*, $P = 0.51$, $P = 0.57$). These data indicate that SO optimum length was found at an imposed SO MTU length of ~ P^A_{ref}+2 mm. The LG+PL reference position, corresponding to 90–90° knee-ankle angles, as well as the MTU lengths imposed in the second protocol were located on the ascending limb of the LG+PL length-force characteristics.

Effects of LG+PL Proximal Position on Distal SO Forces

ANOVA indicated a significant main effect of the position of the proximal LG+PL tendon on both active and passive distal forces of the SO muscle, which was kept at a constant MTU length (Fig. 5). In addition, a significant interaction between the proximal position of LG+PL and the distal position of LG+PL+SO on SO force was found. Repositioning the proximal LG+PL tendon from P^K_{ref}−3 mm to P^K_{ref}+3 mm resulted in an increase of SO force, which was maximally 0.15 N for active and 0.011 N for passive SO. These force increments correspond to 12% and 56% of the active and passive SO force measured at P^K_{ref}, respectively, which is 10% and 0.8% of SO maximal active force. Bonferroni post hoc pairwise comparisons indicated a significant change in passive as well as active SO force compared with SO force at P^K_{ref} when the LG+PL proximal tendon was repositioned by only 1 mm,

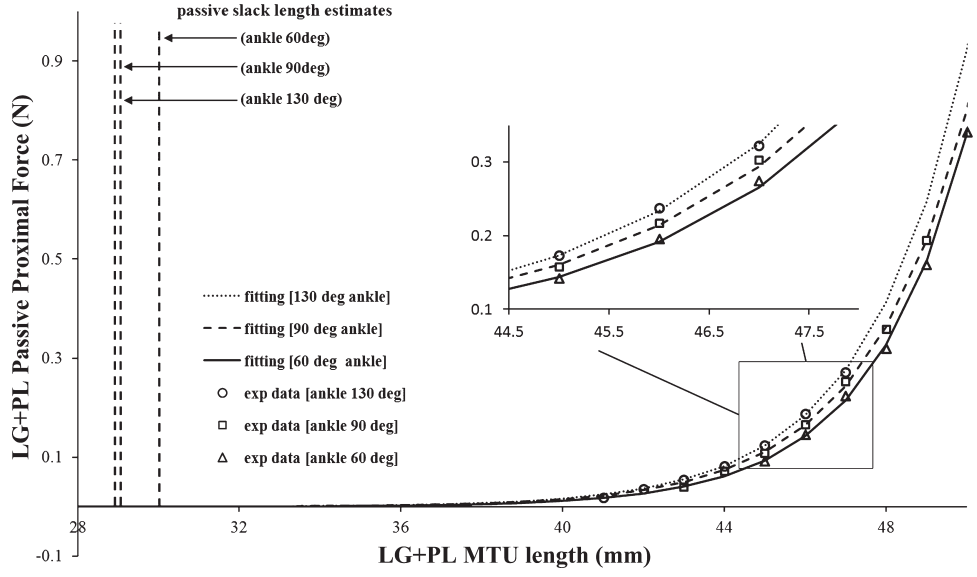

Fig. 3. Assessment of length-passive force characteristics of LG+PL. LG+PL proximal passive forces for a single animal. The dataset obtained for different distal positions of the LG+PL+SO tendons is fitted with exponential functions (see *Eq. 1* in METHODS). The vertical dashed lines indicate the LG+PL passive slack length estimates for each of the 3 different length-force curves. Repositioning of the distal LG+PL and SO tendons [from reference length (L_{ref})−2 mm to L_{ref} +2 mm] correspond to dorsiflexion of the ankle from 60 to 130°. The slack-length estimates were defined as the zero-force level by taking into account a $5*10^{-5}$ N/mm threshold (~0.05% of the measured maximal passive force).

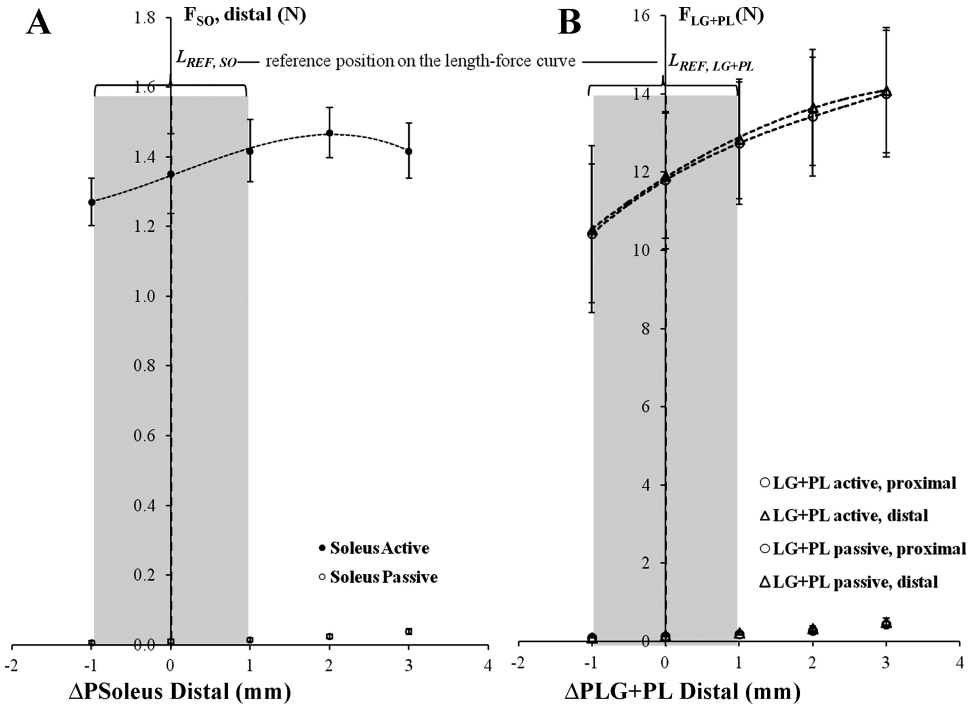

Fig. 4. Active and passive length-force characteristics of SO (*A*) and LG+PL (*B*). Force data are plotted as a function of SO and LG+PL MTU lengths expressed as the deviation relative to the ankle reference position P^{A}_{ref}. The increase in muscle length was obtained by changing the position of the distal tendons of LG+PL and SO (see Fig. 2). The proximal tendon of LG+PL was kept at P^{K}_{ref}, corresponding to a knee angle of 90°. The shaded area represents maximum variation in the position of $L_{ref.}$ Experimental data points of SO and LG+PL active forces are fitted with third order polynomials. Values are shown as means ± SD (n = 9). F_SO, soleus force; F_LG+PL, lateral gastrocnemius and plantaris force; L_REF,SO, soleus muscle-tendon unit length at reference position (or SO MTU length at REF); L_REF_LG+PL, lateral gastrocnemius and plantaris muscle-tendon unit length at reference position (or LG+PL MTU length at REF).

corresponding to a 10–15° knee joint flexion or extension. At the highest MTU lengths tested corresponding to maximum ankle dorsiflexion (P^{A}_{ref}+2 mm), repositioning the LG+PL proximal tendon to maximum knee extension (P^{K}_{ref}+3 mm) caused a small (9.2 ± 8.1 mN) but significant (P = 0.010) decrease in SO active force. These results indicate significant mechanical interactions between active synergistic muscles for in vivo lengths and relative positions. The interaction effect indicates that the extent of force transmitted between SO and LG+PL is affected by the MTU length of SO.

Effects of SO Muscle Relative Position on LG+PL Length-Force Characteristics

The length-force characteristics (Fig. 6) measured at the proximal and distal tendons of LG+PL overlap at three lengths (L = 42, 43, and 44 mm) where LG+PL was kept at the same MTU length but the SO muscle was at a different length and relative position (i.e., most distally at P^{A}_{ref}−2 mm and most proximally at P^{A}_{ref}+2 mm). ANOVA revealed a significant main effect of SO relative position on LG+PL forces, both

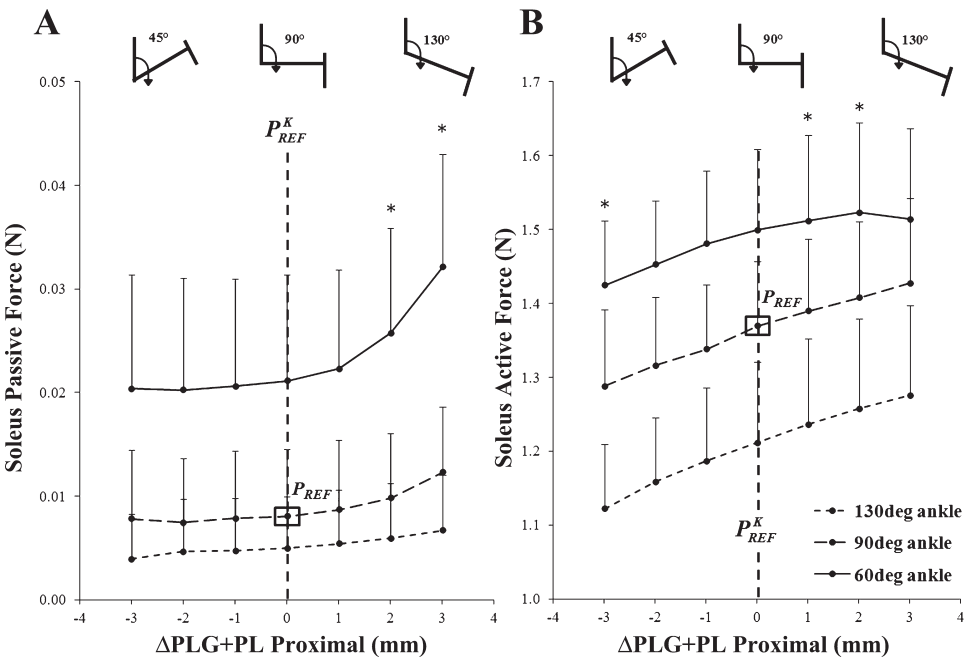

Fig. 5. Effects of lengthening LG+PL proximally on soleus forces. Passive (*A*) and active (*B*) forces exerted at the distal tendon of SO (means + SD, n = 9) plotted as a function of the position of the LG+PL proximal tendon (ΔP) from P^{K}_{ref}−3 to P^{K}_{ref}+3 mm. The corresponding simulated knee angles are showed above. This relationship was assessed for 3 different simulated ankle configurations (from P^{A}_{ref} −2 to P^{A}_{ref}+2 mm for LG+PL+SO distal tendons, corresponding to an ankle-angle range from 60 to 130°). LG+PL proximal position (ΔP) is expressed as the deviation from the position corresponding to a 90° knee angle. Significant force increments compared with the SO force at ΔP = 0 (P^{K}_{ref}) are shown (*P < 0.05).

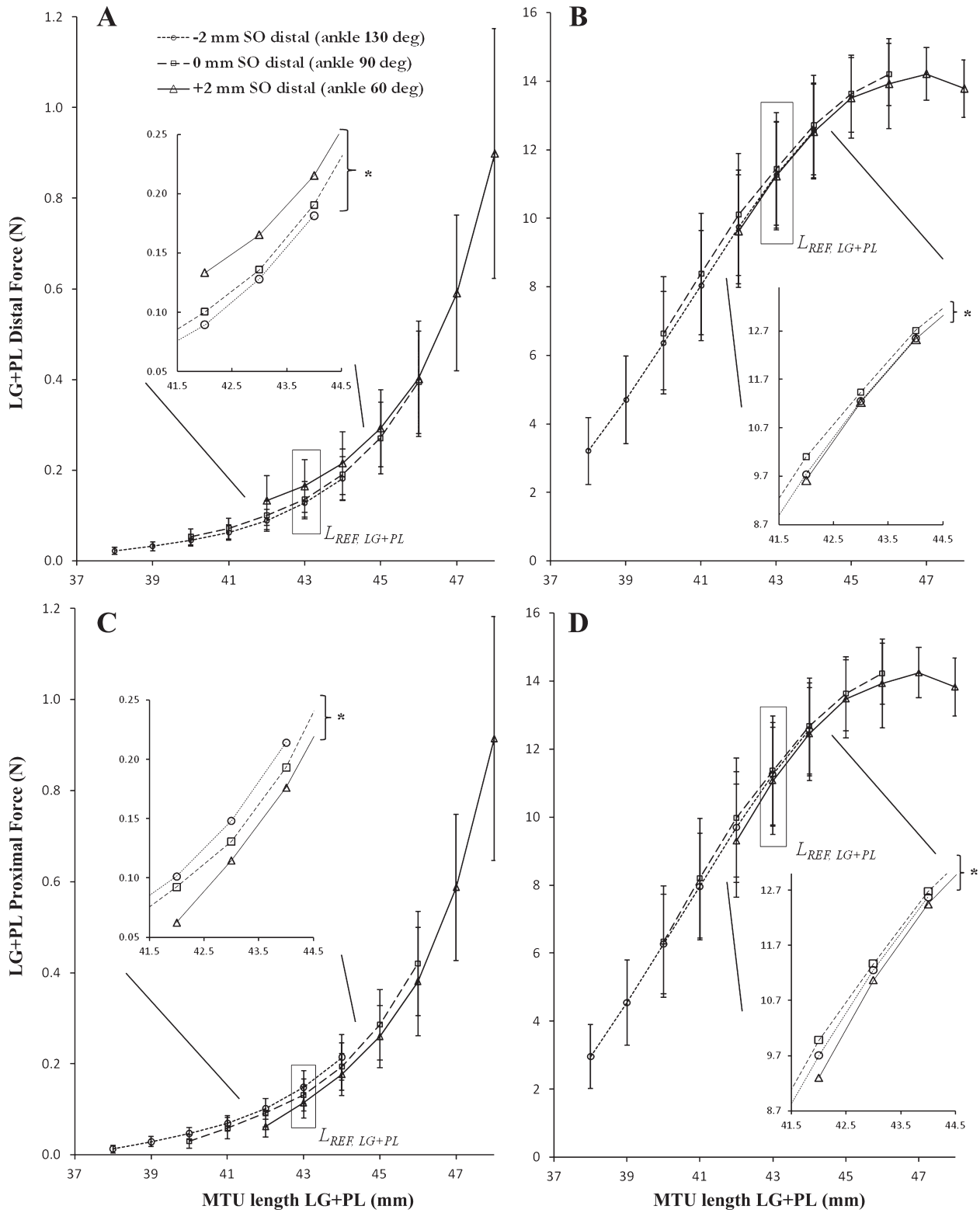

Fig. 6. LG+PL length-force characteristics for different relative positions of SO. Passive (*A* and *C*) and active (*B* and *D*) forces exerted at the distal and proximal tendons of LG+PL (means ± SD, $n = 9$) plotted as a function of its MTU length for 3 different simulated ankle positions (○ 130°, □ 90°, △ 60°). The same MTU length provided significantly different passive as well as active isometric forces of LG+PL depending on the relative position of SO (from $P^{A}_{ref}-2$ mm to $P^{A}_{ref}+2$ mm, $*P < 0.05$). Each graph includes a magnified selection of the area in which 3 data points of LG+PL proximal and distal forces at equal MTU length ($L_{LG+PL} = 42, 43, 44$ mm), but with different lengths and relative positions of the SO muscle measured. Passive forces measured at the same MTU length decreased with increasing ankle joint angle (*A*) and increased with increasing ankle joint angles (*C*). Differences between proximally and distally measured LG+PL forces were not significant for those lengths at which multiple data points were available ($P = 0.071$ active LG+PL, $P = 0.11$ passive LG+PL).

Table 1. *Maximal RMSE between estimated length-force curves*

	RMSE, mN*	%†
Passive, proximal	62.5 ± 25.1	44.2
Passive, distal	78.0 ± 60.7	50.3
Active, proximal	1,124.5 ± 652.8	9.5
Active, distal	785.8 ± 497.8	6.6

Values are means ± SD (%) RMSE between the LG+PL fitted passive and active length-force curves. *The comparison between the curves obtained either with the proximally or distally measured LG+PL tendon forces are reported separately. RMSE values are obtained comparing curve pairs after the fitting procedure. †Percentage of the mean measured LG+PL force at LG+PL reference length ($L_{ref,LG+PL}$).

proximally and distally. For each of these LG+PL lengths, isometric LG+PL forces were not equal. Passive length-force curves of distal LG+PL were shifted toward lower force levels with increasing ankle angles (Fig. 6*A*), but toward higher force levels with increasing ankle angles for proximal LG+PL (Fig. 6*C*). However, differences between proximal and distal LG+PL forces were not significant for the considered subset of data points ($P = 0.071$, active forces; $P = 0.11$, passive forces). The maximum RMSE (passive: 0.08 ± 0.06 N; active 0.79 ± 0.49 N) between the three length-force curves was up to 50% of LG+PL force measured at $L_{ref,LG+PL}$ (Table 1). These results indicate that LG+PL length-force characteristics are not unique but are dependent on the relative position of SO.

Effects of SO muscle relative position on estimates of LG+PL muscle properties. The estimated passive slack length varied between 1 and 3 mm (on average 8.7% of the mean passive slack length estimate within the same animal) due to changes in SO muscle relative position (Table 2). The passive slack length estimate varied between 2 and 5 mm (on average 14.6% of the mean estimate within the same animal) as a result of differences between proximally and distally measured LG+PL forces. Estimated maximal active force of LG+PL varied by 0.69 ± 1.0 N (4.8%) among the length-force curves obtained for the three different SO relative positions. The variation in maximal active force estimates based on LG+PL force exerted proximally or distally was 0.24 ± 0.14 N (1.6%). On average across SO muscle relative positions and location of LG+PL force measurement, the variation in optimum length estimates was smaller than 3 mm for all animals tested (on average 0.5 ± 1.0 mm). Thus estimation of key parameters of LG+PL length-force characteristics is affected by the relative position of SO, with passive slack length varying the most.

DISCUSSION

The most important and novel finding in this study is that SO and LG+PL muscles transmit forces at their muscle belly interface within a physiological range of muscle length and relative positions. This result confirms our hypothesis that epimuscular myofascial force transmission is present within the rat triceps surae muscle group in a functional subset of muscle conditions.

Functionally Relevant Effects of Epimuscular Myofascial Force Transmission

This is the first study reporting the effects of mechanical interaction between SO muscle and two synergists via epimuscular myofascial pathways in the rat over a physiological range of muscle lengths and relative positions. Because SO is a single-joint muscle, the force it can exert is commonly assumed to depend solely on its distal tendon position, varying with ankle-joint angle. In contrast, our results show that manipulating the position of the proximal LG+PL tendon, as associated with knee extension, causes a significant increase in SO passive and active forces. This finding is consistent with previous evidence of mechanical interactions between various muscles in the rat (for a review see Ref. 16). Earlier in situ studies in the rat have found 5–52% changes in the active force exerted by a restrained synergist when lengthening an agonistic muscle by 9–14 mm (15, 19, 31, 40, 41, 44, 47, 64). However, the MTU lengths involved in those studies were beyond the physiological operating range and a single muscle was changed length distally, yielding unphysiological muscle relative positions. Our results indicate that significant but generally smaller (12% of active SO force with knee and ankle at 90°) degrees of mechanical interaction can be observed between SO and LG+PL if tested within the constraints of normal movement (i.e., 6 mm lengthening LG+PL proximally).

Using the same synergistic muscle group as the present study, Maas and Sandercock (35) investigated EMFT for physiological muscle lengths and relative positions in a nearly intact cat hindlimb. Ankle moments of SO muscle were measured at various knee (70–140°) and ankle (50–100°) angles: under these conditions, no effect of EMFT on the moment exerted by SO muscle was found, despite the evidence of strong connective tissue linkages between these muscles (35). Our results contradict those findings, proving the existence of mechanical interaction between SO and LG+PL within their functional range. Several factors may explain these opposite results: *1*) In our study, the distal LG+PL and SO tendons

Table 2. *Variability range between estimates of passive slack length, maximal active force, and optimum length*

Estimates		Variability range, mean ± SD*	%†
Passive slack length, mm	SO relative position	2.1 ± 0.7	5.3
	proximal-distal LG+PL	2.9 ± 1.1	14.6
Maximal active force, mN	SO relative position	699.1 ± 1,074	4.8
	proximal-distal LG+PL	244.3 ± 144.6	1.6
Optimum length, mm	SO relative position	0.5 ± 1.0	1.2
	proximal-distal LG+PL	0.3 ± 0.5	0.7

*Variability ranges were evaluated from the reconstructed passive and active lateral gastrocnemius and plantaris complex (LG+PL) length-force characteristics. The range of variation for muscle properties estimates was calculated depending on the relative position of soleus (SO) and on the difference between proximally and distally measured LG+PL forces. †Percentage of the mean calculated estimate among the 3 fitted curves for each animal.

were separated, whereas in the cat study these tendons merge into the intact Achilles tendon. Effects of EMFT may be counteracted by effects of a common elasticity (56): lengthening LG+PL proximally, thus increasing force at the distal tendon of SO, can result in a higher length of the Achilles tendon and shortening of the SO muscle belly. *2*) There may be differences in stiffness of the epimuscular linkages between species, but such differences have not yet been characterized. *3*) In contrast to our study, in the experiment by Maas and Sandercock, SO muscle was excited exclusively. In such a condition, there is no active force produced by gastrocnemius and plantaris muscle fibers to be transmitted to SO. This suggests that only active gastrocnemius and plantaris muscles can affect force exerted at the distal tendon of SO.

Although a physiologically relevant range of MTU lengths was applied and these muscles are active simultaneously during normal movements (48), several nonphysiological factors were still involved in the present study. Firstly, we excited the muscle maximally whereas during most tasks muscle activation is submaximal and it has already been shown that effects of EMFT are significantly affected by firing rate (40). Secondly, to measure forces exerted by the SO and those exerted by the LG separately, it was required to separate their distal tendons. In an intact limb both tendons merge to the Achilles tendon. Thirdly, simplifications and assumptions involved in the biomechanical model (18) used to translate joint angles to translational tendon positions may introduce inaccuracies in the physiological range of lengths and relative positions set for the present experiment. By using a subset of joint angle ranges (ankle: 60–130°, knee: 45–130°, included angles), we expect such errors to be minimal. Finally, our focus on the SO and LG+PL interface required resection of the surrounding muscles, namely medial gastrocnemius and biceps femoris, as well as separation of the superficial posterior compartment. This approach allowed us to quantify the interaction between the targeted muscles exclusively. However, any possible force pathway between the whole muscle group and the surrounding tissues via extramuscular connections was discarded a priori. Potential mechanical interactions with those structures as well as with antagonist muscles may occur in vivo and affect force transmission to the distal tendons of SO and LG+PL (15, 33, 47).

Assessment of Length-Force Characteristics of Human Biarticular Muscles

We found significantly different LG+PL forces exerted at the same MTU length as a result of changes in the relative position of SO. This has important implications for the experimental techniques used to determine length-force characteristics in humans in vivo. A critical assumption for this approach is that the force produced by a muscle depends on muscle length and activation level only. Considering the gastrocnemius muscle, this implies that dorsiflexion of the ankle should shift up the gastrocnemius length-moment curve in a parallel fashion, because only force exerted by the one-joint SO is expected to change (see for example Fig. 3 in 11). In contrast, nonparallel gastrocnemius length-ankle moment curves have been reported for different ankle joint angles (22). Note that none of the other studies using this method (12, 60, 61) show the actual raw MTU length-moment data to verify parallelism. Our results show that the assumption of mechanical independency is not valid for the rat plantar flexors. Accordingly, values of length-force curve parameters span a relatively large range of solutions dependent on the relative position of the one-joint muscle and the location of force measurement, i.e., proximal or distal (Table 1). The effects of EMFT may partially explain the previously reported variability when reconstructing length-force curves for human muscles. A 3–6% RMSE error between the passive length-force curves measured on the same day and 1 wk apart have been reported (12). In another study, an estimated 4–7% random sampling error was found (60). Because it is not possible to control the relative position of neighboring muscles during in vivo measurements in humans, we conclude that those data can be subjected to contamination due to effects of EMFT.

Mechanisms of Mechanical Interaction between Synergistic Muscles

The force changes measured at the distal SO tendon as a result of lengthening LG+PL proximally can be explained by two mechanisms: *1*) direct transmission of force generated by LG+PL muscle fibers via the connective tissue network to the distal tendon of SO and *2*) effects of myofascial loads on the sarcomere length within SO and LG+PL, as predicted by using finite element models (67). In agreement with this second explanation, we observed a significant decrease in SO distal active force occurring at the highest imposed muscle lengths for LG+PL and SO (Fig. 5*B*, $P^{A}_{ref}+2$ mm, corresponding to a 60° ankle angle). The active length-force characteristics of SO indicate that this condition (Fig. 4, $L_{ref,SO}+2$ mm) corresponds to a MTU length close to its optimum. The observed SO distal force decrease, with increasing LG+PL length proximally, is therefore consistent with SO fibers being stretched beyond optimum by intermuscular linkages, while the overall MTU length of SO was kept constant. As predicted with use of a 3D finite-element model including intermuscular connective tissue linkages, proximal and distal force difference can cause an uneven strain distribution between sarcomeres located proximally and distally within muscle fibers (66). However, the experimental approach exploited here does not allow to distinguish whether SO force changes are caused by SO sarcomere lengths affected by myofascial loads or direct transmission of LG+PL force.

Implications of In Vivo EMFT for Human Function and Pathology

Our results confirm that synergistic muscles are mechanically interdependent when operating within their normal context. However, the extent of EMFT should be carefully evaluated to assess the implications for normal function in humans. An ultrasound study on human subjects found no effects of knee angle on pennation angle and fascicle length of passive and active SO (24). In addition, the relationship between fascicle length and MTU length of medial gastrocnemius muscle was found to be similar at different knee and ankle joint angles (13), also suggesting mechanical interaction with SO to be negligible. Our present results contradict these findings, because differences in LG+PL passive and active forces were observed at equal MTU lengths. Also the findings of several imaging studies in humans indicate that the functional output

of healthy neighboring muscles and muscle groups is partially determined by their relative positions. Changes in SO fascicle (43) and muscle belly length (4) upon stimulation of only medial gastrocnemius have been reported. In addition, passive knee joint movement was found to cause local length changes or displacements of SO muscle (4, 21, 55). These findings suggest that EMFT can play a role in vivo, and thus the central nervous system has to take this into account in the neural control of movement, for instance during a sit-to-stand task, which involves a relatively large knee extension with minimal ankle joint movement (6). Considering the human hand, the fingers are not independent from each other in terms of movement and force production (8, 25, 27, 46). Such coupling has been explained by neural factors but also by mechanical factors (57, 58). With regard to the latter, predominantly connections between the tendons of the extrinsic muscles have been considered (25, 28, 59). However, also myofascial linkages between the heads of extrinsic muscles may play a role (34). In fact, there is evidence of mechanical interaction via EMFT between the long flexor of the thumb and the other digits (63).

Considering pathological conditions in which connective tissues are stiffer than normal, subsequent changes in the magnitude of forces transmitted between muscles may explain alterations in the functional output of the affected muscles. Scar tissue formation following muscle-tendon injury has been associated with a reduction in the range of muscle tissue displacement and strain (50, 51). In addition, EMFT has been discussed as a potential cause of movement limitations in spastic paresis (15) and as a codeterminant of muscle functional output after tendon transfer surgeries in patients with spastic cerebral palsy (53). In fact, previous experiments in the rat that used different muscle preparations to assess the effects of tenotomy and aponeurotomy on the target and neighboring muscles (1, 20, 30, 65) suggest that epimuscular connective tissues may affect joint neutral position and range of movement after surgery. Also, scar tissue formation and merging of donor muscles with adjacent structures were found as long-term effects of hamstring tendon harvesting for anterior cruciate ligament reconstruction (54), which may relate to the variable outcomes of such surgeries. The above illustrates the functional relevance of EMFT in healthy as well as pathological conditions of our muscular system.

Conclusions

We found mechanical interactions between rat ankle plantar flexors for physiological positions of their muscle bellies and for MTU lengths corresponding to a range of motion of the ankle and knee joints found during normal movements. We conclude that isometric muscle force is determined not only by MTU length, but also by the relative position of the neighboring synergists. An important implication of these results is that frequently obtained muscle parameters, such as passive slack and optimum length, cannot be described by a single value for skeletal muscles within their in vivo context.

GRANTS

This study was supported by Division for Earth and Life Sciences of the Netherlands Organization for Scientific Research to H. Maas (864-10-011).

DISCLOSURES

No conflicts of interest, financial or otherwise, are declared by the author(s).

AUTHOR CONTRIBUTIONS

M.B., J.H.v.D., and H.M. conception and design of research; M.B. and G.C.B. performed experiments; M.B. analyzed data; M.B., J.H.v.D., and H.M. interpreted results of experiments; M.B. prepared figures; M.B. drafted manuscript; M.B., J.H.v.D., and H.M. edited and revised manuscript; M.B., J.H.v.D., G.C.B., and H.M. approved final version of manuscript.

REFERENCES

1. **Ateş F, Özdeşlik RN, Huijing PA, Yucesoy CA.** Muscle lengthening surgery causes differential acute mechanical effects in both targeted and non-targeted synergistic muscles. *J Electromyogr Kinesiol* 23: 1199–1205, 2013.
2. **Bauman JM, Chang YH.** High-speed X-ray video demonstrates significant skin movement errors with standard optical kinematics during rat locomotion. *J Neurosci Methods* 186: 18–24, 2010.
3. **Bobbert MF, Ettema GC, Huijing PA.** The force-length relationship of a muscle-tendon complex: experimental results and model calculations. *Eur J Appl Physiol Occup Physiol* 61: 323–329, 1990.
4. **Bojsen-Moller J, Schwartz S, Kalliokoski KK, Finni T, Magnusson SP.** Intermuscular force transmission between human plantarflexor muscles in vivo. *J Appl Physiol* 109: 1608–1618, 2010.
5. **Canu MH, Garnier C.** A 3D analysis of fore- and hindlimb motion during overground and ladder walking: comparison of control and unloaded rats. *Exp Neurol* 218: 98–108, 2009.
6. **Doorenbosch CAM, Harlaar J, Roebroeck ME, Lankhorst GJ.** Two strategies of transferring from sit-to-stand; the activation of monoarticular and biarticular muscles. *J Biomech* 27: 1299–1307, 1994.
7. **Gillis GB, Biewener AA.** Hindlimb muscle function in relation to speed and gait: in vivo patterns of strain and activation in a hip and knee extensor of the rat (Rattus norvegicus). *J Exp Biol* 204: 2717–2731, 2001.
8. **Hager-Ross C, Schieber MH.** Quantifying the independence of human finger movements: comparisons of digits, hands, and movement frequencies. *J Neurosci* 20: 8542–8550, 2000.
9. **Herbert RD, Hoang PD, Gandevia SC.** Are muscles mechanically independent? *J Appl Physiol* 104: 1549–1550, 2008.
10. **Herzog W, ter Keurs HE.** Force-length relation of in-vivo human rectus femoris muscles. *Pflügers Arch* 411: 642–647, 1988.
11. **Herzog W, ter Keurs HE.** A method for the determination of the force-length relation of selected in-vivo human skeletal muscles. *Pflügers Arch* 411: 637–641, 1988.
12. **Hoang PD, Gorman RB, Todd G, Gandevia SC, Herbert RD.** A new method for measuring passive length-tension properties of human gastrocnemius muscle in vivo. *J Biomech* 38: 1333–1341, 2005.
13. **Hoang PD, Herbert RD, Todd G, Gorman RB, Gandevia SC.** Passive mechanical properties of human gastrocnemius muscle tendon units, muscle fascicles and tendons in vivo. *J Exp Biol* 210: 4159–4168, 2007.
14. **Hoy MG, Zajac FE, Gordon ME.** A musculoskeletal model of the human lower extremity: the effect of muscle, tendon, and moment arm on the moment-angle relationship of musculotendon actuators at the hip, knee, and ankle. *J Biomech* 23: 157–169, 1990.
15. **Huijing PA.** Epimuscular myofascial force transmission between antagonistic and synergistic muscles can explain movement limitation in spastic paresis. *J Electromyogr Kinesiol* 17: 708–724, 2007.
16. **Huijing PA.** Epimuscular myofascial force transmission: a historical review and implications for new research. International Society of Biomechanics Muybridge Award Lecture, Taipei, 2007. *J Biomech* 42: 9–21, 2009.
17. **Huijing PA.** Muscular force transmission necessitates a multilevel integrative approach to the analysis of function of skeletal muscle. *Exerc Sport Sci Rev* 31: 167–175, 2003.
18. **Huijing PA, Baan GC.** Extramuscular myofascial force transmission within the rat anterior tibial compartment: proximo-distal differences in muscle force. *Acta Physiol Scand* 173: 297–311, 2001.
19. **Huijing PA, Baan GC.** Myofascial force transmission via extramuscular pathways occurs between antagonistic muscles. *Cells Tissues Organs* 188: 400–414, 2008.
20. **Huijing PA, Baan GC, Rebel GT.** Non-myotendinous force transmission in rat extensor digitorum longus muscle. *J Exp Biol* 201: 683–691, 1998.
21. **Huijing PA, Yaman A, Ozturk C, Yucesoy CA.** Effects of knee joint angle on global and local strains within human triceps surae muscle: MRI analysis indicating in vivo myofascial force transmission between synergistic muscles. *Surg Radiol Anat* 33: 869–879, 2011.

22. **Huijing PA, Yucesoy CA, Baan GC, Maas H.** Implications of muscle relative position as a co-determinant of isometric muscle force. *J Mech Med Biol* 03: 145–168, 2003.
23. **Johnson WL, Jindrich DL, Roy RR, Reggie Edgerton V.** A three-dimensional model of the rat hindlimb: musculoskeletal geometry and muscle moment arms. *J Biomech* 41: 610–619, 2008.
24. **Kawakami Y, Ichinose Y, Fukunaga T.** Architectural and functional features of human triceps surae muscles during contraction. *J Appl Physiol* 85: 398–404, 1998.
25. **Kilbreath SL, Gandevia SC.** Limited independent flexion of the thumb and fingers in human subjects. *J Physiol* 479: 487–497, 1994.
26. **Kreulen M, Smeulders MJC, Hage JJ, Huijing PA.** Biomechanical effects of dissecting flexor carpi ulnaris. *J Bone Joint Surg Br* 85-B: 856–859, 2003.
27. **Lang CE, Schieber MH.** Human finger independence: limitations due to passive mechanical coupling versus active neuromuscular control. *J Neurophysiol* 92: 2802–2810, 2004.
28. **Linburg RM, Comstock BE.** Anomalous tendon slips from the flexor pollicis longus to the flexor digitorum profundus. *J Hand Surg Am* 4: 79–83, 1979.
29. **Lloyd DG, Besier TF.** An EMG-driven musculoskeletal model to estimate muscle forces and knee joint moments in vivo. *J Biomech* 36: 765–776, 2003.
30. **Maas H, Baan GC, Huijing PA.** Dissection of a single rat muscle-tendon complex changes joint moments exerted by neighboring muscles: implications for invasive surgical interventions. *PloS One* 8: e73510, 2013.
31. **Maas H, Baan GC, Huijing PA.** Intermuscular interaction via myofascial force transmission: effects of tibialis anterior and extensor hallucis longus length on force transmission from rat extensor digitorum longus muscle. *J Biomech* 34: 927–940, 2001.
32. **Maas H, Baan GC, Huijing PA.** Muscle force is determined also by muscle relative position: isolated effects. *J Biomech* 37: 99–110, 2004.
33. **Maas H, Huijing PA.** Synergistic and antagonistic interactions in the rat forelimb: acute effects of coactivation. *J Appl Physiol* 107: 1453–1462, 2009.
34. **Maas H, Jaspers RT, Baan GC, Huijing PA.** Myofascial force transmission between a single muscle head and adjacent tissues: length effects of head III of rat EDL. *J Appl Physiol* 95: 2004–2013, 2003.
35. **Maas H, Sandercock TG.** Are skeletal muscles independent actuators? Force transmission from soleus muscle in the cat. *J Appl Physiol* 104: 1557–1567, 2008.
36. **Maas H, Sandercock TG.** Force transmission between synergistic skeletal muscles through connective tissue linkages. *J Biomed Biotechnol* 2010: 575672, 2010.
37. **MacIntosh BR, MacNaughton MB.** The length dependence of muscle active force: considerations for parallel elastic properties. *J Appl Physiol* 98: 1666–1673, 2005.
38. **Maganaris CN.** Force-length characteristics of the in vivo human gastrocnemius muscle. *Clin Anat* 16: 215–223, 2003.
39. **Magnuson DS, Smith RR, Brown EH, Enzmann G, Angeli C, Quesada PM, Burke D.** Swimming as a model of task-specific locomotor retraining after spinal cord injury in the rat. *Neurorehabil Neural Repair* 23: 535–545, 2009.
40. **Meijer HJM, Rijkelijkhuizen JM, Huijing PA.** Effects of firing frequency on length-dependent myofascial force transmission between antagonistic and synergistic muscle groups. *Eur J Appl Physiol* 104: 501–513, 2008.
41. **Meijer HJM, Rijkelijkhuizen JM, Huijing PA.** Myofascial force transmission between antagonistic rat lower limb muscles: effects of single muscle or muscle group lengthening. *J Electromyogr Kinesiol* 17: 698–707, 2007.
42. **Nordez A, Foure A, Dombroski EW, Mariot JP, Cornu C, McNair PJ.** Improvements to Hoang et al.'s method for measuring passive length-tension properties of human gastrocnemius muscle in vivo. *J Biomech* 43: 379–382, 2010.
43. **Oda T, Kanehisa H, Chino K, Kurihara T, Nagayoshi T, Fukunaga T, Kawakami Y.** In vivo behavior of muscle fascicles and tendinous tissues of human gastrocnemius and soleus muscles during twitch contraction. *J Electromyogr Kinesiol* 17: 587–595, 2007.
44. **Olesen AT, Jensen BR, Uhlendorf TL, Cohen RW, Baan GC, Maas H.** Muscle-specific changes in length-force characteristics of the calf muscles in the spastic Han-Wistar rat. *J Appl Physiol* 117: 989–997, 2014.
45. **Purslow PP.** Muscle fascia and force transmission. *J Bodyw Mov Ther* 14: 411–417, 2010.
46. **Reilly KT, Hammond GR.** Independence of force production by digits of the human hand. *Neurosci Lett* 290: 53–56, 2000.
47. **Rijkelijkhuizen JM, Meijer HJ, Baan GC, Huijing PA.** Myofascial force transmission also occurs between antagonistic muscles located within opposite compartments of the rat lower hind limb. *J Electromyogr Kinesiol* 17: 690–697, 2007.
48. **Roy RR, Hutchison DL, Pierotti DJ, Hodgson JA, Edgerton VR.** EMG patterns of rat ankle extensors and flexors during treadmill locomotion and swimming. *J Appl Physiol* 70: 2522–2529, 1991.
49. **Sandercock TG.** Nonlinear summation of force in cat soleus muscle results primarily from stretch of the common-elastic elements. *J Appl Physiol* 89: 2206–2214, 2000.
50. **Silder A, Heiderscheit BC, Thelen DG, Enright T, Tuite MJ.** MR observations of long-term musculotendon remodeling following a hamstring strain injury. *Skeletal Radiol* 37: 1101–1109, 2008.
51. **Silder A, Reeder SB, Thelen DG.** The influence of prior hamstring injury on lengthening muscle tissue mechanics. *J Biomech* 43: 2254–2260, 2010.
52. **Smeulders MJ, Kreulen M, Hage JJ, Huijing PA, van der Horst CM.** Spastic muscle properties are affected by length changes of adjacent structures. *Muscle Nerve* 32: 208–215, 2005.
53. **Smeulders MJC, Kreulen M.** Myofascial force transmission and tendon transfer for patients suffering from spastic paresis: a review and some new observations. *J Electromyogr Kinesiol* 17: 644–656, 2014.
54. **Snow BJ, Wilcox JJ, Burks RT, Greis PE.** Evaluation of muscle size and fatty infiltration with MRI nine to eleven years following hamstring harvest for ACL reconstruction. *J Bone Joint Surg Am* 94: 1274–1282, 2012.
55. **Tian M, Herbert RD, Hoang P, Gandevia SC, Bilston LE.** Myofascial force transmission between the human soleus and gastrocnemius muscles during passive knee motion. *J Appl Physiol* 113: 517–523, 2012.
56. **Tijs C, van Dieën J, Baan GC, Maas H.** Three-dimensional ankle moments and nonlinear summation of rat triceps surae muscles. *PLoS One* 9: e111595, 2014.
57. **van Duinen H, Gandevia SC.** Constraints for control of the human hand. *J Physiol* 589: 5583–5593, 2011.
58. **van Duinen H, Yu WS, Gandevia SC.** Limited ability to extend the digits of the human hand independently with extensor digitorum. *J Physiol* 587: 4799–4810, 2009.
59. **von Schroeder HP, Botte MJ.** The functional significance of the long extensors and juncturae tendinum in finger extension. *J Hand Surg Am* 18: 641–647, 1993.
60. **Winter SL, Challis JH.** The force-length curves of the human rectus femoris and gastrocnemius muscles in vivo. *J Appl Biomech* 26: 45–51, 2010.
61. **Winter SL, Challis JH.** Reconstruction of the human gastrocnemius force-length curve in vivo: part 2-experimental results. *J Appl Biomech* 24: 207–214, 2008.
62. **Yaman A, Ozturk C, Huijing PA, Yucesoy CA.** Magnetic resonance imaging assessment of mechanical interactions between human lower leg muscles in vivo. *J Biomech Eng* 135: 91003, 2013.
63. **Yu WS, Kilbreath SL, Fitzpatrick RC, Gandevia SC.** Thumb and finger forces produced by motor units in the long flexor of the human thumb. *J Physiol* 583: 1145–1154, 2007.
64. **Yucesoy CA, Baan G, Huijing PA.** Epimuscular myofascial force transmission occurs in the rat between the deep flexor muscles and their antagonistic muscles. *J Electromyogr Kinesiol* 20: 118–126, 2010.
65. **Yucesoy CA, Huijing PA.** Substantial effects of epimuscular myofascial force transmission on muscular mechanics have major implications on spastic muscle and remedial surgery. *J Electromyogr Kinesiol* 17: 664–679, 2007.
66. **Yucesoy CA, Koopman BFJM, Huijing PA, Grootenboer HJ.** Finite element modeling of intermuscular interactions and myofascial force transmission. In: *Engineering in Medicine and Biology Society, 2001. Proceedings of the 23rd Annual International Conference of the IEEE* (vol. 2). Piscataway, NJ: IEEE/EMB, 2001, p. 1201–1204, vol. 1202.
67. **Yucesoy CA, Koopman BH, Grootenboer HJ, Huijing PA.** Finite element modeling of aponeurotomy: altered intramuscular myofascial force transmission yields complex sarcomere length distributions determining acute effects. *Biomech Model Mechanobiol* 6: 227–243, 2007.